MRI characterization of ex vivo healthy human lymph nodes at 7T

M. A. Korteweg[1], J. J. Zwanenburg[1], P. van Diest[2], I. H. Borel Rinkes[3], W. P. Mali[1], P. R. Luijten[1], and W. B. Veldhuis[1]

[1]Radiology, University Medical Center Utrecht, Utrecht, Netherlands, [2]Pathology, University Medical Center Utrecht, Utrecht, Netherlands, [3]Surgery, University Medical Center Utrecht, Utrecht, Netherlands

Introduction: Breast cancer is the most common form of cancer in women worldwide. Axillary lymph node status is the most important factor determining prognosis. Assessment of nodal status currently requires surgical resection. First a partial dissection is performed, which, if positive (for metastasis), is followed by a complete axillary lymph node dissection (ALND). These procedures are associated with morbidity and, in retrospect, are often performed unnecessarily. Institutional Review Board approval has been obtained for the upcoming start of a prospective, dual center trial comparing non-invasive 3T MR imaging-based staging to surgical staging of the axillary lymph nodes. The performance of the in vivo MRI will be controlled by 7T ex vivo MRI of all surgical specimens. This will be followed by a node-to-node matching of all imaged nodes with pathology. The aim is to detect (micro) metastases by analyzing morphology and relaxation times of the metastatic and non-metastatic areas of the dissected nodes at 7T. Subsequent pathologic examination is the gold standard. This abstract describes the evaluation of the 7T scan protocol and the pathological matching. Furthermore the initial results of 7T MRI characterization of normal human lymph nodes are presented and correlated with pathology.

Material and Methods: Two ALNDs, performed by an experienced surgeon, were retrieved during autopsy of an otherwise healthy female who died of a heart attack. The ALNDs were stitched onto a plastic rack, in order to maintain a consistent shape, and were conserved in formaldehyde. During 7T MRI scanning (Philips Health Care, Cleveland, USA), using a Transmit/Receive head coil with a 16 channel receive coil (Nova Medical Systems), the specimens were submersed in fomblin to provide susceptibility matching. The scan protocol consisted of a 3D T2 weighted fat suppressed fast field echo (fsFFE) [TR/TE 158/5.59ms, flipangle 35º, FOV 23.6x110x110mm, resolution 0.18mm isotropic], a T1-map which was obtained with a 2D Look-Locker sequence [TR (between inversions) 4000ms, TE 3.72ms, flipangle 3º, FOV 5x110x110mm, in plane resolution 0.5mm, 100 samples with an increment of 40ms, initial TI 18ms], a 3D T2-map which was obtained from a multi-echo spin echo sequence [TR/first TE/ΔTE 13618/30/30ms, 8 echoes, FOV 24x110x110mm, resolution 0.5mm isotropic], a 3D T2*-map which was obtained from a multi-echo gradient echo sequence [TR/first TE/ΔTE 136/4.96/4.96ms, 10 echoes, flipangle 30º, FOV 24x110x110mm, resolution 0.5mm isotropic] and a multi-slice diffusion weighted image [TR/TE 4000/74.1ms, FOV 24x110x110mm, slice thickness 0.7mm, in plane resolution 0.7mm, b-values 0, 750 and 1500s/mm^2]. The mean absolute T1, T2 and T2* relaxation times and the apparent diffusion coefficients (ADC) were determined for all lymph nodes based on hand-drawn regions of interest. Pathological processing as well as final pathological examination were performed by an experienced pathologist. To maintain an accurate correlation of MRI with pathology, the superior and one lateral side of each node were dyed black and blue respectively, and a numbered map of each ALND specimen was drawn, detailing the location and shape of each node. The nodes were then excised from the surrounding fat and sliced in 4mm sections and numbered again. They were paraffin embedded and cut into 3µm thick slices which were stained with Haematoxylin & Eosin (H&E).

Table 1. 7T relaxation times, and ADC of healthy human lymph nodes; from ALND1 and ALND2.

		ALND 1	ALND 2
T1	Mean (±SD)	1481.00 (82.36)ms	1293.44 (147.27)ms
T2*	Mean (±SD)	17.46 (3.6)ms	19.31 (11.06)ms
T2	Mean (±SD)	72.05 (15.35)ms	72.04 (13.80)ms
ADC	Mean (±SD)	$0.35 \cdot 10^{-3}$ (0.12) s/mm^2	$0.44 \cdot 10^{-3}$ (0.1)s/mm^2

Results: On MRI 13 nodes were detected in total. All 13 nodes were also retrieved during the routine analysis of the ALND performed by the pathologist. No additional nodes were found. Table 1 shows the lymph node relaxation times and ADC for the two specimens. On MRI afferent lymph vessels and efferent blood- and lymph vessels were identified, as were multiple B-cell follicles (diameter range 0.4-1.5mm) situated in the periphery of the lymph nodes. These MR findings were correlated with the results of pathology, which showed normal reactive lymph nodes with small follicles ranging up to 1.3mm in diameter. Not every node was entirely dissected into 3µm sections, which probably explains the discrepancy in size measurements of the detected follicles between MRI and pathology.

Conclusion & Discussion: 7T MRI of ex vivo human lymph nodes correlates well with pathology. The same number of nodes were detected by MRI as by subsequent histological sectioning. The developed protocol for specimen-handling achieves a precise correlation of the imaged nodes with pathology. Preliminary ADC values and 7T relaxation times were determined for, pathologically-confirmed, healthy lymph nodes. The imaging protocol has shown to provide very high resolution images, allowing identification of perinodal lymph- and blood vessels as well as intranodal B-cell follicles. These structural details are relevant because perinodal vessels increase in number and B-cell follicles can increase in size in case of (pending) metastasis. We hope that the current set up will aid us in matching in vivo imaged lymph nodes to pathology in the upcoming clinical trial. Also this will hopefully increase our understanding of imaging changes detected in vivo in breast cancer patients.

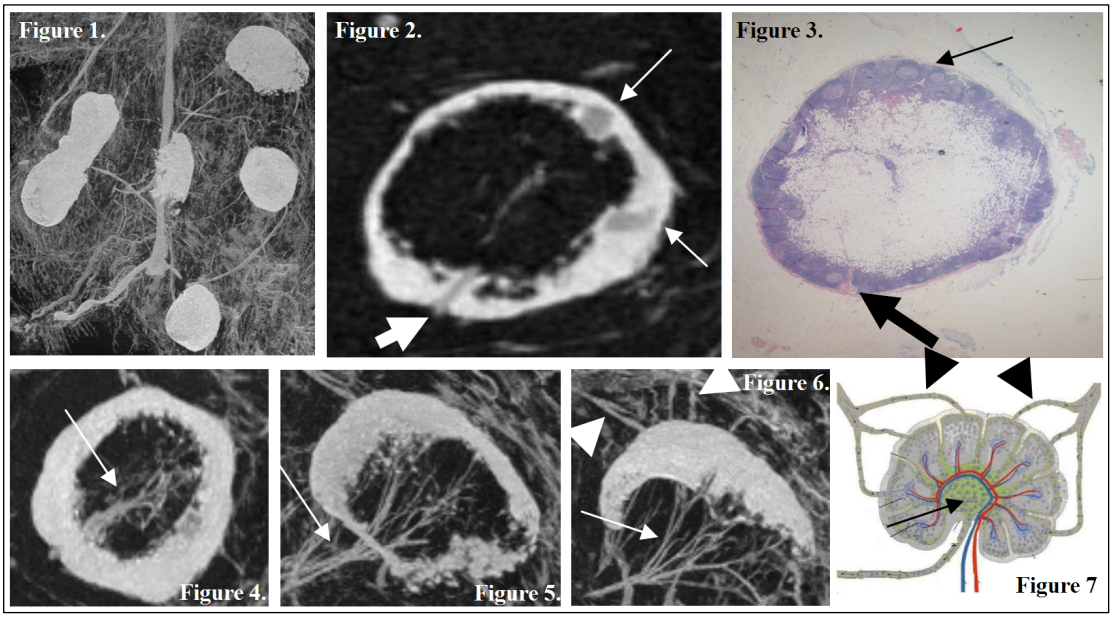

Fig. 1. Maximum intensity projection (MIP) of a 3D T2W-fsFFE of ALND1, showing 6 lymph nodes (white "balls") against a background of suppressed fat. **Fig. 2.** 0.18mm slice through one of the lymph nodes shown on Fig. 1. Several B-cell follicles (thin arrows) and a vessel (fat arrow) are visible. **Fig. 3.** Microscopic view of a H&E stained 3µm section of the lymph node shown on Fig. 2. The fat arrow indicates the same vessel as in Fig. 2. Several B-cell follicles are visible (thin arrow). The fatty center of the node corresponds to the suppressed background in Fig 2. **Figs 4-6.** Thin-slab MIPs of a 3D T2W-fsFFE, through several nodes shown on Fig. 1. Indicated are afferent lymphatic vessels entering at the cortical convexity (arrow heads) and efferent vessels at the concave side of the nodes (thin arrows). **Fig. 7** Drawing corresponding to Figs 4-6.